

Carbazole-bis(oxazolines) as Monoanionic, Tridentate Chelates in Lanthanide Chemistry: Synthesis and Structural Studies of Thermally Robust and Kinetically Stable Dialkyl and Dichloride Complexes.

Jin Zou,[†] David J. Berg,^{*,†} David Stuart,[†] Robert McDonald,[‡] and Brendan Twamley[§]

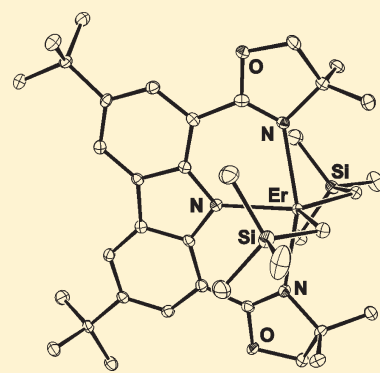
[†]Department of Chemistry, University of Victoria, P.O. Box 3065 Victoria, British Columbia V8W 3V6, Canada

[‡]X-ray Crystallography Laboratory, Department of Chemistry, University of Alberta, Edmonton, Alberta T6G 2G2, Canada

[§]Department of Chemistry, University of Idaho, P.O. Box 442343, Moscow, Idaho 83844-2343, United States

S Supporting Information

ABSTRACT: The carbazole-bis(oxazoline) ligand 1,8-bis(4',4'-dimethyloxazolin-2'-yl)-3,6-di-*tert*-butylcarbazole (H-Czx, **14**) was prepared and reacted with $\text{Ln}(\text{CH}_2\text{SiMe}_3)_3(\text{THF})_2$ to afford the five-coordinate dialkyl complexes $(\text{Czx})\text{Ln}(\text{CH}_2\text{SiMe}_3)_2$ ($\text{Ln} = \text{Y}$, **15**; Er, **16**; Yb, **17**) in high yield. Deprotonation of **14** with $\text{NaN}(\text{SiMe}_3)_2$, followed by reaction with $\text{LnCl}_3(\text{THF})_{x_1}$ affords the six-coordinate dichloride complexes *cis,mer*- $(\text{Czx})\text{Ln}(\text{Cl})_2(\text{THF})$ ($\text{Ln} = \text{Y}$, **18**; Er, **19**; Yb, **20**). Dialkyl complexes **15**–**17** were also prepared by reaction of the dichloride complexes **18**–**20**, respectively, with 2 equiv of $\text{LiCH}_2\text{SiMe}_3$. Complexes **16**–**20** were characterized by X-ray crystallography. The dialkyl complexes **16** and **17** display a five-coordinate trigonal-bipyramidal geometry with the Czx ligand spanning both axial and one equatorial site with the CH_2SiMe_3 rotated such that the SiMe_3 groups sit over the carbazole ring system. The solution structure for **15**–**20** was found to be consistent with that in the solid state by NMR spectroscopy. However, paramagnetic dichloride **20** was shown by variable-temperature ^1H NMR studies to undergo rapid THF exchange by a dissociative process in toluene- d_8 solution ($\Delta H^\ddagger = 98 \pm 10 \text{ kJ mol}^{-1}$, $\Delta S^\ddagger = +185 \pm 25 \text{ J mol}^{-1} \text{ K}^{-1}$). Treatment of dialkyl **18** with $[\text{Ph}_3\text{C}]^+[\text{B}(\text{C}_6\text{F}_5)_4]^-$ cleanly produces the alkyl cation $[(\text{Czx})\text{Y}(\text{CH}_2\text{SiMe}_3)]^+[\text{B}(\text{C}_6\text{F}_5)_4]^-$ (**21**) by ^1H NMR spectroscopy, but this species does not insert 2,3-dimethylbutadiene.



INTRODUCTION

Oxazolines ligands have been extensively used in transition metal coordination chemistry for many years.¹ Easy access to these ligands by condensation of amino alcohols with carboxylic acid derivatives or nitriles allows straightforward modification of the ligand architecture including the incorporation of chirality when chiral amino alcohols, derived from readily available amino acids, are used. Enantioselective synthesis based on pybox ligands (Chart 1, **1**) is one particularly well-established example of oxazoline-derived ligand systems in current use.² In contrast to their extensive use in transition metal chemistry, relatively few lanthanide complexes containing coordinated oxazoline rings have been reported, and most of these are neutral ligand systems (e.g., **1**–**4**, Chart 1) that are not especially suited to these metals. Despite this, lanthanide and group 3 complexes of **1**–**4** have proven successful as asymmetric catalysts in many reactions.³ A few lanthanide complexes of anionic ligands containing oxazolines as part of the architecture (**5**–**7**, Chart 2) have been reported,⁴ but only ligand **7**^{4a} has been applied to lanthanide organometallic chemistry.

Our interest in these ligands stems from the fact that oxazoline rings coordinate almost exclusively as hard σ -donors through the imino nitrogen, but the $\text{C}=\text{N}$ linkage remains inert to attack by strong nucleophiles such as carbanions. The fact that the steric bulk of the oxazoline is readily tunable is an important advantage

in lanthanide chemistry. Despite its obvious attractions, the oxazoline ring system is neutral and therefore likely to suffer from high lability when coordinated to a lanthanide metal center. However, attaching two oxazolines to a carbazole-based core gives a tridentate, monoanionic carbazole-bis(oxazoline) (Czx) chelate that should be well suited to organolanthanide chemistry. In addition to being strongly anchored through the carbazole amido nitrogen, the rigid, planar nature of the chelate array should enforce a well-defined *mer* coordination geometry at the metal ion.

Chiral carbazole-bis(oxazoline) ligands (**8**, Chart 3) were originally developed by Nakada and Inoue for use in the asymmetric Nozaki–Hiyama allylation, allenylation, and propargylation of aldehydes using Cr^{2+} complexes of these ligands formed *in situ* as catalysts.⁵ More recently, Connell has extended this chemistry to the synthesis of butadien-2-ylcarbinols, also using Cr^{2+} Czx complexes as catalysts.⁶ It should also be noted that transition metal complexes of related carbazole-bis(imino)⁷ and carbazole-bis(pyridine)⁸ ligands have been previously reported (Chart 3, **9** and **10**, respectively). To our knowledge, Czx ligands have not been previously used in lanthanide chemistry, but a Y^{3+} dialkyl complex of a carbazole-bis(phosphine), **11**, and a Lu^{3+} dialkyl

Received: July 4, 2011

Published: August 24, 2011

Chart 1

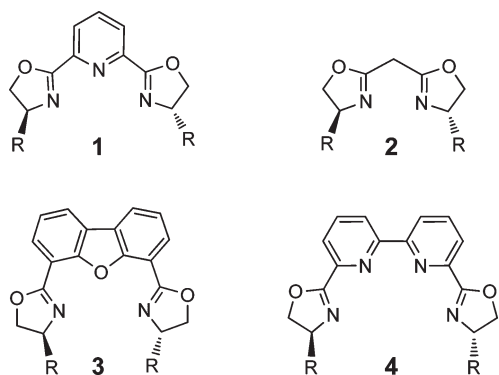
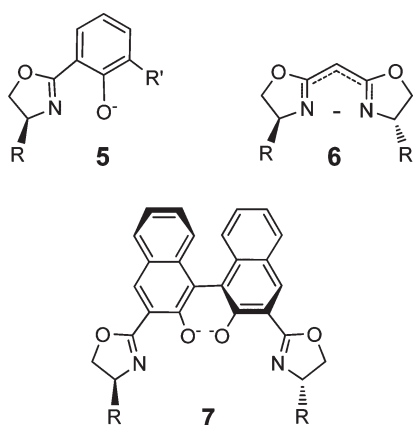


Chart 2



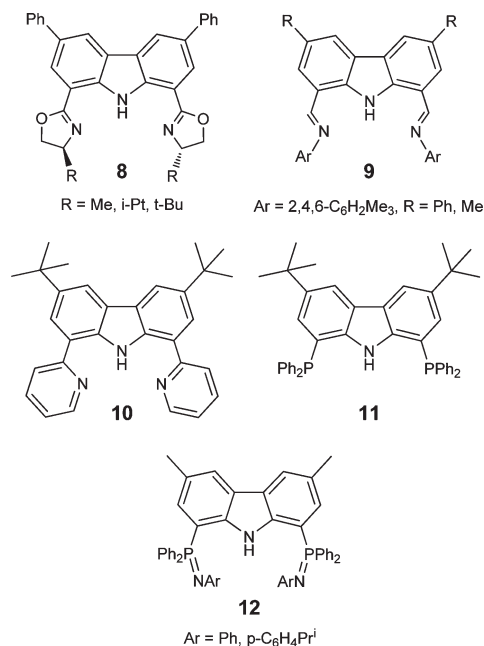
complex of the closely related carbazole-bis(phosphinimine), **12**, have very recently been reported.⁹ In this contribution, we show that the carbazole-bis(oxazoline) ligand allows easy access to five-coordinate lanthanide dialkyl and six-coordinate lanthanide dichloride complexes that exhibit remarkable stability to thermal degradation and ligand redistribution.

EXPERIMENTAL SECTION

General Procedures. All reactions were done under an argon or nitrogen atmosphere using glovebox (Braun MB150-GII) or Schlenk methods. Tetrahydrofuran (THF) was dried by distillation from sodium benzophenone ketyl under argon immediately before use; other solvents were used directly from an MBraun solvent purification system. Toluene and hexane were stored in the glovebox for prolonged periods over activated 4 Å sieves. Carbazole, CuCN, and *N*-methyl-2-pyrrolidone were purchased from Aldrich and used as received. Anhydrous LnCl₃ salts (Ln = Y, Er, Yb) were purchased from Aldrich and used as received or converted to their THF solvates, LnCl₃(THF)_{*x*} by extraction with anhydrous THF. 3,6-Di-*tert*-butylcarbazole,⁷ 1,8-dibromo-3,6-di-*tert*-butylcarbazole,⁷ Ln(CH₂SiMe₃)₃(THF)₂ (Y, Er, Yb),^{10a–c} and NaN(SiMe₃)₂^{10d} were prepared according to literature procedures.

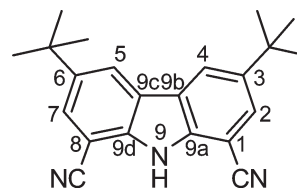
NMR spectra were recorded on a Bruker AMX-500 (¹H, 500 MHz; ¹³C, 125 MHz) or Bruker AMX-360 (¹H, 360 MHz) spectrometer. Benzene-*d*₆ and toluene-*d*₈ were dried over activated 4 Å sieves, and THF-*d*₈ was distilled from sodium benzophenone and stored in the glovebox. Air-sensitive samples for NMR analysis were sealed using a 5 mm tube fitted with a Teflon valve (Brunfeldt). NMR assignments,

Chart 3



where specified, were confirmed by 2D ¹H–¹³C COSY (HMQC, HMBC) experiments on diamagnetic compounds. Mass spectra were recorded on a Kratos Concept H spectrometer using electron impact (70 eV) ionization. Elemental analyses were conducted by Canadian Microanalytical, Delta, BC, or the Department of Chemistry, University of British Columbia. Although repeated attempts were tried, satisfactory analyses of **17**, **18**, and **20** were not obtained. Melting points were carried out in sealed capillary tubes using a Büchi melting point apparatus and are not corrected. Infrared spectra were obtained using KBr discs on a Perkin-Elmer Spectrum One FTIR spectrometer.

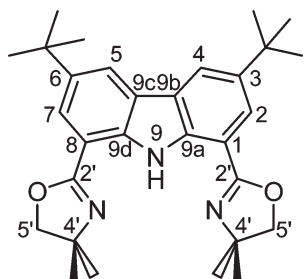
1,8-Dicyano-3,6-di-*tert*-butylcarbazole, **13**.



1,8-Dibromo-3,6-di-*tert*-butylcarbazole⁶ (10.02 g, 22.92 mmol) was dissolved in 180 mL of *N*-methyl-2-pyrrolidone in a foil-covered flask. CuCN (5.33 g, 60 mmol) was added, and the solution was refluxed at 180 °C overnight. After cooling, the solution was poured into a beaker containing 400 mL of ammonium hydroxide and 200 mL of ethyl acetate, and the resulting suspension was stirred for 30 min. The precipitate was filtered through Celite, and the filtrate was extracted with ethyl acetate (5 × 300 mL). The combined organic extracts were washed with concentrated brine (2 × 300 mL) and dried over anhydrous MgSO₄. Filtration, removal of the solvent from the filtrate, and recrystallization of the crude product from ethyl acetate afforded pure **13**. Yield: 6.04 g (80%). Mp: 287–290 °C. ¹H NMR (500 MHz, CDCl₃, 298 K): δ 9.92 (s, 1H, NH), 8.29 (d, *J* = 1.8 Hz, 2H, 4,5-arylH), 7.82 (d, *J* = 1.8 Hz, 2H, 2,7-arylH), 1.43 (s, 18H, C(CH₃)₃). ¹³C{¹H} NMR (125 MHz, CDCl₃): δ 144.02 (3,6-arylC), 139.36 (9a,9d-arylC), 128.70 (2,7-arylC), 123.99

(9b,9c-arylC), 122.33 (4,5-arylC), 117.24 (CN), 94.33 (1,8-arylC), 35.12 (C(CH₃)₃), 31.92 (C(CH₃)₃). EI-MS: *m/z* 329 (M⁺).

1,8-Bis(4',4'-dimethyloxazolin-2'-yl)-3,6-di-tert-butylcarbazole (H-Czx), 14.



1,8-Dicyano-3,6-di-tert-butylcarbazole, **13** (2.00 g, 6.07 mmol), was dissolved in 100 mL of chlorobenzene along with 2-methyl-2-aminopropanol (1.62 g, 18.2 mmol) and anhydrous ZnCl₂ (2.08 g, 15.3 mmol). The reaction mixture was refluxed for 72 h and then cooled to room temperature. The reaction mixture was poured into a solution of ethylenediamine (10 mL) and water (100 mL) and stirred for 1 h. The resulting biphasic solution was extracted with CH₂Cl₂ (3 × 100 mL), and the combined organic layers were washed with brine (2 × 100 mL) and dried over anhydrous MgSO₄. After the filtration, the organic layer evaporated to dryness and the residue was purified by column chromatography on silica using CH₂Cl₂ as eluant. Pure H-Czx, **13**, was isolated as a white powder (1.15 g, 40%). Mp: 278–280 °C. ¹H NMR (500 MHz, CDCl₃, 298 K): δ 11.87 (s, 1H, NH), 8.19 (d, *J* = 1.8 Hz, 2H, 4,5-arylH), 7.89 (d, *J* = 1.8 Hz, 2H, 2,7-arylH), 4.16 (s, 4H, CH₂), 1.47 (s, 12H, 4'-(CH₃)₂), 1.45 (s, 18H, C(CH₃)₃). ¹³C{¹H} NMR (125 MHz, CDCl₃): δ 161.27 (C=N), 141.34 (3,6-arylC), 137.61 (9a,9d-arylC), 123.18 (9b,9c-arylC), 122.65 (2,7-arylCH), 119.56 (4,5-arylCH), 109.66 (1,8-arylC), 78.32 (CH₂), 67.55 (4'-C(CH₃)₂), 34.68 (C(CH₃)₃), 32.26 (C(CH₃)₃), 28.84 (4'-C(CH₃)₂). IR (KBr): ν 3336 (br s), 2961, 1648, 1490, 1363, 1286, 1152, 727, 668 cm⁻¹. EI-MS: *m/z* 473 (M⁺). Anal. Calcd for C₃₀H₃₉N₃O₂: C 76.08, H 8.30, N 8.87. Found: C 75.66, H 8.28, N 8.77.

(Czx)Y(CH₂SiMe₃)₂, 15. In the glovebox, Y(CH₂SiMe₃)₃(THF)₂ (0.49 g, 1.0 mmol) was dissolved in 10 mL of toluene in a 50 mL Erlenmeyer flask. A solution of H-Czx (0.47 g, 1.0 mmol) in 5 mL of toluene was added by pipet, resulting in an immediate color change to neon yellow. After 2 h at room temperature, the solvent was removed under reduced pressure using a rotary evaporator, and the solid residue obtained was recrystallized from a mixture of toluene and hexane to afford **15** as pale yellow crystals (0.66 g, 90%). Mp: 196 °C (dec). ¹H NMR (500 MHz, C₆D₆, 298 K): δ 8.65 (d, *J* = 2.2 Hz, 2H, 4,5-arylH), 8.51 (d, *J* = 1.8 Hz, 2H, 2,7-arylH), 3.72 (s, 4H, CH₂), 1.56 (s, 12H, 4'-(CH₃)₂), 1.39 (s, 18H, C(CH₃)₃), 0.04 (s, 18H, Si(CH₃)₃), 0.00 (s, *J*_{Y,H} = 2.6 Hz, 4H, CH₂Si(CH₃)₃). ¹³C{¹H} NMR (125 MHz, CDCl₃): δ 170.28 (C=N), 148.05 (9a,9d-arylC), 140.78 (3,6-arylC), 127.84 (9b,9c-arylC), 126.46 (2,7-arylCH), 123.31 (4,5-arylCH), 109.76 (1,8-arylC), 79.09 (CH₂), 69.14 (4'-C(CH₃)₂), 37.46 (*J*_{Y,C} = 38.5 Hz, CH₂Si(CH₃)₃), 35.01 (C(CH₃)₃), 32.30 (C(CH₃)₃), 27.89 (4'-C(CH₃)₂), 4.76 (Si(CH₃)₃). IR (KBr): ν 2956, 1634, 1596, 1472, 1362, 1176, 861, 776, 668 cm⁻¹. This compound decomposed after several hours at room temperature in the glovebox so an elemental analysis was not obtained.

(Czx)Er(CH₂SiMe₃)₂, 16. This complex was prepared on the same scale and using the same procedure reported for **15** above. Yellow cubes of **16** were isolated by recrystallization from a toluene–hexane mixture.

Yield: 0.77 g (92%). Mp: 206 °C (dec). ¹H NMR (360 MHz, C₆D₆, 298 K): δ 81.2 (s, 12H, ν_{1/2} = 567 Hz, 4'-(CH₃)₂), 76.5 (s, 4H, ν_{1/2} = 158 Hz, CH₂), 42.9 (s, 2H, ν_{1/2} = 75 Hz, 2,7-arylH), 7.26 (s, 2H, ν_{1/2} = 20 Hz, 4,5-arylH), 6.45 (s, 18H, ν_{1/2} = 17 Hz, C(CH₃)₃), -62.2 (s, 18H, ν_{1/2} = 154 Hz, Si(CH₃)₃), -185.0 (s, 4H, ν_{1/2} = 2360 Hz, CH₂Si(CH₃)₃). IR (KBr): ν 2955, 1635, 1576, 1476, 1363, 1176, 852, 730, 668 cm⁻¹. Anal. Calcd for C₃₈H₆₀N₃O₂Si₂Er: C 56.05, H 7.43, N 5.16. Found: C 56.52, H 7.38, N 5.29.

(Czx)Yb(CH₂SiMe₃)₂, 17. This complex was prepared on the same scale and using the same procedure reported for **15** above. Orange-red cubes of **17** were isolated by recrystallization from a toluene–hexane mixture. Yield: 0.75 g (91%). Mp: 250 °C (dec). ¹H NMR (360 MHz, C₆D₆, 298 K): δ 69.2 (s, 16H, ν_{1/2} = 59 Hz, 4'-(CH₃)₂ and CH₂), 33.5 (s, 2H, ν_{1/2} = 18 Hz, 2,7-arylH), 2.61 (s, 18H, ν_{1/2} = 6 Hz, C(CH₃)₃), -1.60 (s, 2H, ν_{1/2} = 9 Hz, 4,5-arylH), -39.9 (s, 18H, ν_{1/2} = 26 Hz, Si(CH₃)₃), -174.8 (s, 4H, ν_{1/2} = 54 Hz, CH₂Si(CH₃)₃). IR (KBr): ν 2954, 1634, 1575, 1476, 1363, 1176, 852, 730, 668 cm⁻¹. Anal. Calcd for C₃₈H₆₀N₃O₂Si₂Yb: C 55.65, H 7.37, N 5.12. Found: C 52.60, H 6.28, N 5.60. The crystals changed color from orange-red to yellow when exposed to high vacuum.

(Czx)Y(Cl)₂(THF), 18. YCl₃(THF)_x (0.45 g, 1.0 mmol) was partially dissolved in 10 mL of THF in a 50 mL Erlenmeyer flask in the glovebox. A solution of NaCzx (0.50 g, 1.0 mmol) in 5 mL of THF was prepared *in situ* by deprotonation of H-Czx, **14** (0.48 g, 1.0 mmol), with 1 equiv of Na[N(SiMe₃)₂] (0.18 g, 1.0 mmol). The NaCzx solution was added to the YCl₃(THF)_x suspension dropwise by Pasteur pipet, resulting in an immediate color change to neon yellow-green. After 1 h at room temperature, the reaction mixture was filtered through Celite to remove NaCl, and the solvent was removed from the filtrate under reduced pressure using a rotary evaporator. Crude **18** was recrystallized from benzene to afford yellow-green crystals of pure **18**. Yield: 0.63 g (90%). Mp: 272 °C (dec). ¹H NMR (500 MHz, C₆D₆, 298 K): δ 8.54 (d, *J* = 2.2 Hz, 2H, 4,5-arylH), 8.48 (d, *J* = 2.1 Hz, 2H, 2,7-arylH), 3.53 (s, 4H, CH₂), 3.38 (t, 4H, α-CH₂ THF), 1.76 (s, 12H, 4'-(CH₃)₂), 1.45 (s, 18H, C(CH₃)₃), 0.72 (t, 4H, β-CH₂ THF). ¹³C{¹H} NMR (125 MHz, C₆D₆): δ 169.04 (C=N), 147.58 (9a,9d-arylC), 140.57 (3,6-arylC), 127.57 (9b,9c-arylC), 126.77 (2,7-arylCH), 123.31 (4,5-arylCH), 110.23 (1,8-arylC), 79.85 (CH₂), 69.34 (4'-C(CH₃)₂), 35.05 (C(CH₃)₃), 32.43 (C(CH₃)₃), 28.45 (4'-C(CH₃)₂). Anal. Calcd for C₄₆H₅₈Cl₂N₃O₃Y: C 64.25, H 6.75, N 4.89. Found: C 64.45, H 6.87, N 4.98.

(Czx)Er(Cl)₂(THF), 19. This complex was prepared on the same scale and using the same procedure reported for **18** above. Yellow crystals of **19** were isolated by recrystallization from a toluene–hexane mixture. Yield: 0.74 g (95%). Mp: 270 °C (dec). ¹H NMR (360 MHz, C₆D₆, 298 K): δ 41.9 (s, 16H, ν_{1/2} = 2730 Hz, 4'-(CH₃)₂ and CH₂), 20.2 (s, 2H, ν_{1/2} = 1080 Hz, 2,7-arylH), 0.80 (s, 18H, ν_{1/2} = 60 Hz, C(CH₃)₃), -2.44 (s, 2H, ν_{1/2} = 34 Hz, 4,5-arylH), -14.1 (s, 4H, ν_{1/2} = 114 Hz, β-THF), -30.6 (s, 4H, ν_{1/2} = 578 Hz, α-THF). Anal. Calcd for C₄₆H₅₈Cl₂N₃O₃Er: C, 58.96, H 6.20, N 4.49. Found: C 57.80, H 5.86, N 4.66.

(Czx)Yb(Cl)₂(THF), 20. This complex was prepared on the same scale and using the same procedure reported for **18** above. Yellow-green crystals of **20** were isolated by recrystallization from a toluene–hexane mixture. Yield: 0.73 g (93%). Mp: 270 °C (dec). ¹H NMR (360 MHz, C₆D₆, 298 K): δ 49.3 (s, 4H, ν_{1/2} = 670 Hz, CH₂), 43.8 (s, 12H, ν_{1/2} = 680 Hz, 4'-(CH₃)₂), 20.0 (s, 2H, ν_{1/2} = 102 Hz, 2,7-arylH), -0.97 (s, 18H, ν_{1/2} = 6 Hz, C(CH₃)₃), -8.63 (s, 2H, ν_{1/2} = 26 Hz, 4,5-arylH), -9.6 (s, 4H, ν_{1/2} = 42 Hz, β-CH₂ THF), -26.0 (s, 4H, ν_{1/2} = 266 Hz, α-CH₂ THF). Anal. Calcd for C₄₆H₅₈Cl₂N₃O₃Yb: C 58.46, H 6.14, N 4.45. Found: C 58.23, H 6.39, N 4.41.

[(Czx)Y(CH₂SiMe₃)⁺][B(C₆F₅)₄]⁻, 21. Treatment of a solution of **15** (0.012 g, 0.016 mmol) dissolved in toluene-*d*₈ (0.6 mL) with 1 equiv of Ph₃C⁺ [B(C₆F₅)₄]⁻ (0.015 g, 0.016 mmol) resulted in an orange-brown solution. This complex decomposed during attempted isolation. The product was characterized *in situ* by NMR spectroscopy in toluene-*d*₈. ¹H NMR

(360 MHz, 298 K): δ 8.53 (d, $J = 1.9$ Hz, 2H, 4,5-arylH), 8.48 (d, $J = 1.9$ Hz, 2H, 2,7-arylH), 7.25–7.28* (m, 6H, *o*-arylH Ph₃CCH₂Si(CH₃)₃), 7.00–7.11* (m, 9H, *m,p*-arylH Ph₃CCH₂Si(CH₃)₃), 3.65 (s, 4H, CH₂), 2.04* (s, 2H, Ph₃CCH₂Si(CH₃)₃), 1.42 (s, 18H, C(CH₃)₃), 1.10 (s, 12H, 4'-(CH₃)₂), 0.07 (d, $^2J_{Y,H} = 2.8$ Hz, 2H, YCH₂Si(CH₃)₃), –0.23 (s, 9H, Si(CH₃)₃), –0.25 (s, 9H, Si(CH₃)₃). $^{13}\text{C}\{^1\text{H}\}$ NMR (90.6 MHz): δ 172.32 (C=N), 149.57 (9a,9d-arylC), 142.96 (3, 6-arylC), 148.8 (dm, $^1J_{\text{CF}} = 238$ Hz, *o*-arylC C₆F₅), 138.5 (dm, $^1J_{\text{CF}} = 246$ Hz, *p*-arylC C₆F₅), 137.0 (dm, $^1J_{\text{CF}} = 247$ Hz, *m*-arylC C₆F₅), 129.01* (*o*-arylCH, Ph₃C), 127.52* (*m*-arylCH, Ph₃C), 127.39 (9b,9c-arylC), 126.50 (2,7-arylCH), 125.86* (*p*-arylCH, Ph₃C), 124.58 (4, 5-arylCH), 108.46 (1,8-arylC), 78.86 (CH₂), 67.67 (4'-C(CH₃)₂), 47.80 (d, $^1J_{Y,C} = 48.8$ Hz, YCH₂Si(CH₃)₃), 35.04 (C(CH₃)₃), 32.11* (Ph₃CCH₂), 31.49 (C(CH₃)₃), 27.13 (4'-C(CH₃)₂), 3.01* (Ph₃CCH₂Si(CH₃)₃), 0.47 (YCH₂Si(CH₃)₃). ^{19}F NMR (282.4 MHz): δ –131.6 (br s, *o*-arylF), –160.4 (t, $^3J_{\text{FF}} = 21$ Hz, *p*-arylF), –164.8 (br s, *m*-arylF). * indicates resonances due to the reaction byproduct, Ph₃CCH₂Si(CH₃)₃.

X-ray Crystallographic Studies. Crystals for analysis were attached to a glass fiber, and data were collected at low temperature (90 K for **16**; 193 K for **17–20**) using a Bruker/Siemens SMART APEX (**16**) or SMART 1000 (**17–20**) instrument (Mo K α radiation, $\lambda = 0.71073$ Å). Data were measured using omega scans 0.3° per frame for 20 s, and a full sphere of data was collected. Data reduction and correction for Lorentz polarization and decay were performed using SAINTPlus software.¹¹ Absorption corrections were applied using SADABS.¹² The structures were solved by direct methods and refined using least-squares on F^2 as implemented in the SHELXTL program package.¹³ All non-hydrogen atoms were refined anisotropically. No significant decomposition was observed during data collection. A summary of the data collection and refinement parameters is given in Table 1. Further details are provided in the Supporting Information.

RESULTS AND DISCUSSION

Synthesis. Reaction of 1 equiv of H-Czx, **14**, with the lanthanide tris(alkyls) Ln(CH₂SiMe₃)₃(THF)₂ afforded the corresponding

THF-free bis(alkyls) (Czx)Ln(CH₂SiMe₃)₂ (Ln = Y (**15**), Er (**16**), Yb (**17**)) in good yields by direct protonolysis (Scheme 1). While this reaction works efficiently for the smaller lanthanides, it does not allow access to the larger members of the series because the tris(alkyl) precursors are unstable for metals larger than samarium. However, the salt metathesis reaction between 1 equiv of Na⁺Czx[–] and LnCl₃(THF)_x cleanly affords the six-coordinate THF solvates (Czx)LnCl₂(THF) (Ln = Y (**18**), Er (**19**), Yb (**20**)), and these can in turn be converted to the corresponding bis(alkyl) complexes **15–17** in good yield (Scheme 1).

Scheme 1

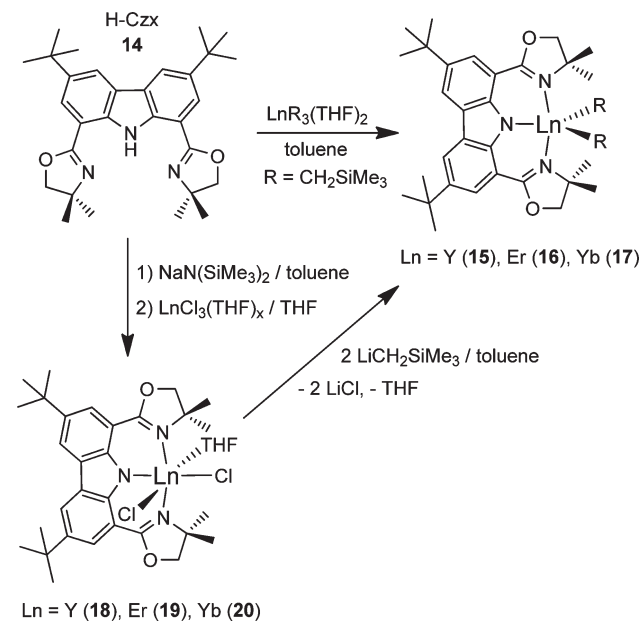


Table 1. Summary of Crystallographic Data

	16^a	17^b	18^b	19^b	20^b
formula	C ₃₈ H ₆₀ ErN ₃ O ₂ Si ₂	C ₃₈ H ₆₀ YbN ₃ O ₂ Si ₂	C ₄₆ H ₅₈ Cl ₂ N ₃ O ₃ Y	C ₄₆ H ₅₈ Cl ₂ ErN ₃ O ₃	C ₄₆ H ₅₈ Cl ₂ N ₃ O ₃ Yb
fw	814.33	820.11	860.76	939.11	944.89
cryst syst	orthorhombic	triclinic	orthorhombic	orthorhombic	orthorhombic
space group	<i>Pna</i> 2 ₁ (No. 33)	<i>P</i> $\bar{1}$ (No. 2)	<i>Pbca</i> (No. 61)	<i>Pbca</i> (No. 61)	<i>Pbca</i> (No. 61)
<i>a</i> (Å)	10.983(4)	14.6863(9)	13.5915(12)	13.5749(7)	13.5448(7)
<i>b</i> (Å)	18.0056(6)	15.5101(10)	17.7957(15)	17.7904(9)	17.7920(9)
<i>c</i> (Å)	20.1636(7)	18.6074(12)	37.215(3)	37.247(2)	37.249(2)
α (deg)	90	80.2013(8)	90	90	90
β (deg)	90	89.0033(9)	90	90	90
γ (deg)	90	89.1795(9)	90	90	90
<i>V</i> (Å ³)	3987.5(2)	4175.8(5)	9001.2(13)	8995.4(8)	8976.7(8)
<i>Z</i>	4	4	8	8	8
ρ_{calc} (g cm ^{–3})	1.356	1.305	1.270	1.387	1.398
μ (mm ^{–1})	2.199	2.329	1.456	2.026	2.244
$2\theta_{\text{max}}$ (deg)	55	55	51	55	55
measd reflns	52 288	36 696	61 378	75 551	75 251
unique reflns	9149	18 922	8438	10 321	10 282
R_i^c , R_w^d	0.024, 0.049	0.033, 0.090	0.050, 0.118	0.033, 0.080	0.034, 0.084
GOF	1.03	1.05	1.03	1.15	1.15

^a Collected using a Bruker/Siemens Smart APEX CCD system (graphite-monochromated Mo K α $\gamma = 0.71073$ Å) at 90 K. ^b Collected using a Bruker Smart 1000 CCD system (graphite-monochromated Mo K α $\gamma = 0.71073$ Å) at 193 K. ^c $R = \Sigma(|F_o| - |F_c|) / \Sigma|F_o|$. ^d $R_w = [\Sigma w(|F_o| - |F_c|)^2] / \Sigma w(|F_o|)^2)^{1/2}$.

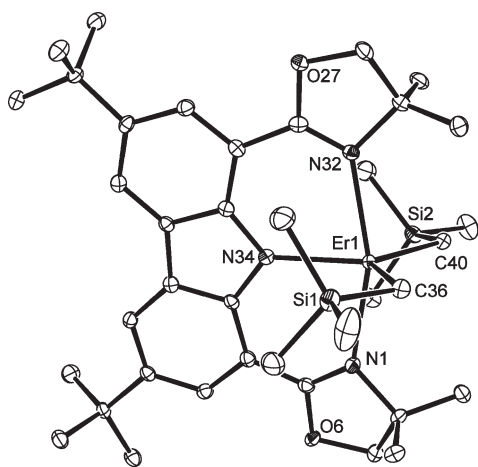


Figure 1. ORTEP³¹⁴ plot (40% probability ellipsoids) of (Czx)Er(CH₂SiMe₃)₂ (**16**).

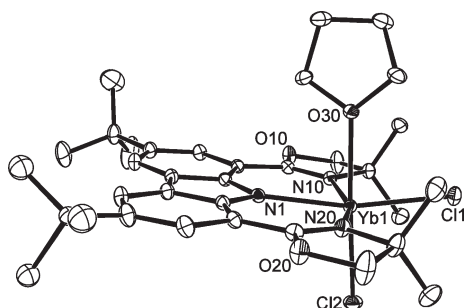


Figure 2. ORTEP³¹⁴ plot (25% probability ellipsoids) of (Czx)Yb(Cl)₂(THF) (**20**).

Structural Studies. The solid-state structures of dialkyl complexes **16** and **17**, as well as the dichloride complexes **18**, **19**, and **20**, were determined by X-ray crystallography. Although erbium dialkyl **16** and ytterbium dialkyl **17** are not isostructural, the coordination geometry is essentially identical in both cases. All three dichloride complexes are isostructural. Table 1 summarizes the crystallographic data for all five structures, while representative ORTEP plots for the dialkyl and dichloride complexes are shown in Figures 1 and 2, respectively. Selected bond lengths and angles for the dialkyl and dichloride complexes are collected in Tables 2 and 3, respectively.

Dialkyl complexes **16** and **17** adopt a monomeric, five-coordinate geometry at the lanthanide center. The geometry at the metal is best described as a distorted trigonal bipyramid with the anionic carbazole N and the alkyl C atoms in the equatorial plane (N_{Cbz}–Ln–C: 117.9(1)°, 121.49(9)° for **16** and 118.54(12)–125.87(11)° for **17**; C–Ln–C: 120.6(1)° for **16** and 109.35(12)°, 117.8(2)° for the two independent molecules in **17**) and the oxazoline N donors in the axial positions (N_{Ox}–Ln–N_{Ox}: 160.55(8)° for **16**; 160.91(9), 160.93(10)° for **17**). Somewhat surprisingly, both alkyl groups in each complex are rotated away from the oxazoline methyl substituents so that they sit over the carbazole ring plane in a “folded wing” geometry. The bend angles at the alkyl C of **16** are among the smallest ever observed in a lanthanide trimethylsilylmethyl complex, and those in **17**, while not quite as acute, are also among the most bent known (Ln–C–Si: **16**, 113.5(2)°, 115.9(1)°; **17**: 117.4(2)°, 118.4(2)°, 118.7(2)°,

Table 2. Selected Bond Lengths and Angles for (Czx)Ln(CH₂SiMe₃)₂ (Ln = Er, **16**; Yb, **17**)^a

	16 (Er)	17 (Yb)	
		molecule A	molecule B
Ln–N _{Ox1}	2.428(2)	2.409(3)	2.404(3)
Ln–N _{Ox2}	2.423(2)	2.416(3)	2.410(3)
Ln–N _{Cbz}	2.312(2)	2.308(2)	2.278(2)
Ln–C ₁	2.398(3)	2.343(3)	2.353(4)
Ln–C ₂	2.404(3)	2.355(3)	2.364(4)
N _{Ox1} –Ln–N _{Ox2}	160.55(8)	160.91(9)	160.93(10)
N _{Ox1} –Ln–N _{Cbz}	80.64(8)	80.73(9)	80.81(9)
N _{Ox1} –Ln–C ₁	95.93(9)	95.49(10)	94.47(14)
N _{Ox1} –Ln–C ₂	94.60(9)	95.40(12)	94.80(14)
N _{Ox2} –Ln–N _{Cbz}	80.23(8)	80.29(8)	80.13(9)
N _{Ox2} –Ln–C ₁	96.11(9)	93.64(10)	95.29(13)
N _{Ox2} –Ln–C ₂	92.35(9)	97.34(11)	95.08(14)
N _{Cbz} –Ln–C ₁	117.9(1)	124.78(10)	118.54(12)
N _{Cbz} –Ln–C ₂	121.49(9)	125.87(11)	123.70(13)
C ₁ –Ln–C ₂	120.6(1)	109.35(12)	117.77(15)
Ln–C ₁ –Si ₁	113.5(2)	120.11(16)	117.36(19)
Ln–C ₂ –Si ₂	115.9(1)	118.72(17)	118.35(19)

^aN_{Ox1}, N_{Ox2}, N_{Cbz}, C₁, and C₂ refer to the following atom labels for **16**: N(1), N(32), N(34), and C(40); for **17** these labels refer to atoms labeled N(10), N(20), N(1), C(1), and C(2), respectively. Si₁ and Si₂ refer to atoms labeled Si(1) and Si(2) in both structures.

Table 3. Selected Bond Lengths and Angles for (Czx)LnCl₂(THF)·2C₆H₆ (Ln = Y, **18**; Er, **19**; Yb, **20**)^a

	18 (Y)	19 (Er)	20 (Yb)
Ln–N _{Ox1}	2.418(3)	2.404(3)	2.391(3)
Ln–N _{Ox2}	2.431(3)	2.418(3)	2.405(3)
Ln–N _{Cbz}	2.331(2)	2.321(3)	2.289(3)
Ln–Cl1	2.6031(10)	2.5911(8)	2.5635(9)
Ln–Cl2	2.5592(10)	2.5442(9)	2.5233(10)
Ln–O _{THF}	2.391(2)	2.390(2)	2.363(2)
N _{Ox1} –Ln–N _{Ox2}	159.59(10)	160.25(9)	161.53(10)
N _{Ox1} –Ln–N _{Cbz}	80.14(9)	80.60(9)	81.18(10)
N _{Ox1} –Ln–Cl1	99.32(7)	99.03(6)	98.55(7)
N _{Ox1} –Ln–Cl2	92.20(7)	92.11(6)	91.91(7)
N _{Ox1} –Ln–O _{THF}	82.78(9)	82.86(8)	83.23(9)
N _{Ox2} –Ln–N _{Cbz}	80.03(10)	80.21(9)	80.89(10)
N _{Ox2} –Ln–Cl1	98.75(7)	98.47(7)	97.91(7)
N _{Ox2} –Ln–Cl2	96.01(8)	95.78(7)	95.40(8)
N _{Ox2} –Ln–O _{THF}	89.87(9)	90.05(9)	90.22(10)
N _{Cbz} –Ln–Cl1	166.13(7)	166.04(7)	166.92(7)
N _{Cbz} –Ln–Cl2	100.10(7)	100.09(7)	99.57(7)
N _{Cbz} –Ln–O _{THF}	82.52(9)	82.49(8)	82.98(9)
Cl1–Ln–Cl2	93.76(4)	93.87(3)	93.50(3)
Cl1–Ln–O _{THF}	83.67(6)	83.62(6)	84.00(7)
Cl2–Ln–O _{THF}	173.89(7)	173.93(6)	174.13(7)

^aN_{Ox1}, N_{Ox2}, N_{Cbz}, and O_{THF} refer to the following atom labels for **18**, **19**, and **20**: N10, N20, N1, and O30; Cl1 and Cl2 refer to the chlorine atoms *trans* and *cis* to the carbazole nitrogen, respectively.

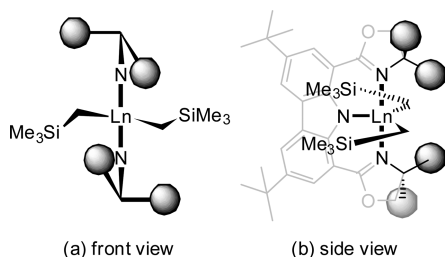


Figure 3. Schematic view showing the disposition of the 4',4'-dimethyl groups of the Czx ligand in the solid-state structure of complexes **16** and **17**.

120.1(2)°; literature:¹⁵ mean = 127°, range 114.4–139.7°. Close inspection of the orientation of the methyl groups on the two oxazoline rings shows that the 4'-carbon is rotated so that one methyl group is about 30° out of the Ln–N–C4' plane (31.9–35.9°), while the other is nearly perpendicular to this plane (88–93°). This allows a staggered arrangement of methyl groups on the two oxazoline rings, but it also forces the trimethylsilylmethyl groups to rotate back over the carbazole plane to avoid strong steric repulsions with the perpendicular methyl groups. The relative arrangement of the oxazoline methyl groups and trimethylsilylmethyl ligands is shown schematically in the cartoon in Figure 3. The small Ln–C–Si angle observed in **16** and **17** places a hydrogen of one methyl group on each trimethylsilyl unit close to the Ln center (Ln···H distance: 3.3 Å). While this is a relatively close contact, it is still outside the sum of the van der Waals radii (3.2 Å),¹⁶ and the ¹J_{CH} coupling constant for this CH₃ is identical to that in Si(CH₃)₄ (¹J_{CH} = 118 Hz), so there is no evidence to support a γ-agostic interaction. The Ln–C bond distances fall well within the normal range for five-coordinate lanthanide trimethylsilyl complexes (distances arbitrarily corrected to reflect Y³⁺ in five-coordination: **16**: 2.408, 2.414 Å; **17**: 2.383, 2.393 Å; literature:^{17,18} mean = 2.39 ± 0.03 Å).

In contrast to the five-coordinate dialkyl complexes **16** and **17**, dichlorides **18**–**20** all coordinate one THF molecule and adopt a six-coordinate, distorted octahedral geometry (Figure 2). Not surprisingly given its rigid, planar structure, the Czx ligand is coordinated in *mer* fashion with the two oxazoline N atoms in *trans*, axial sites (N_{ox}–Ln–N_{ox}: 159.59–161.53°) and the anionic carbazole N in an equatorial position. In all three dichloride structures (**18**–**20**), only the *cis*-dichloride isomer is observed with one chloride *trans* to the carbazole N (N_{Cbz}–Ln–Cl: 166.04–166.92°) and one *trans* to the THF O (O_{THF}–Ln–Cl: 173.89–174.13°). The Ln–N distances for the Cbz ligand are very similar to those observed in the five-coordinate dialkyls **16** and **17**. Given the fact that the average decrease in effective ionic radii across the lanthanide series on going from six- to five-coordination is 0.06 Å,¹⁸ we conclude that the dialkyl complexes are more crowded than the dichlorides, an observation also supported by the absence of coordinated THF in the dialkyls. The terminal Ln–Cl distances fall within the range normally observed for six-coordinate lanthanide dichlorides (2.52–2.62 Å).¹⁹ It is noteworthy, however, that the Ln–Cl bond *trans* to the carbazole N is significantly longer than that *trans* to the THF O in all three cases (Δ in Å: **18**, 0.044; **19**, 0.047; **20**, 0.040). This apparent *trans* influence of the carbazole N could be attributed to steric effects, but the observation that the difference Δ is essentially the same for all three metal ions argues against this and

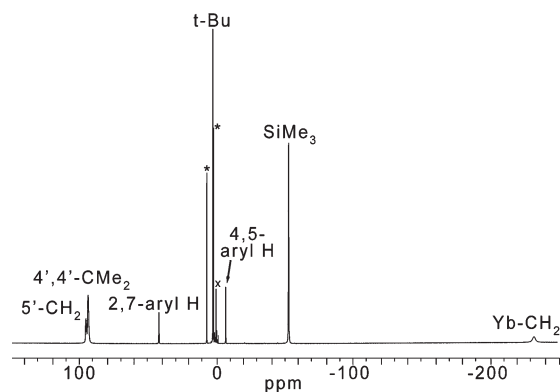


Figure 4. ¹H NMR spectrum (360 MHz, toluene-*d*₈) of (Czx)Yb(CH₂SiMe₃)₂, **17**, at 250 K (*residual solvent resonances; × denotes an impurity).

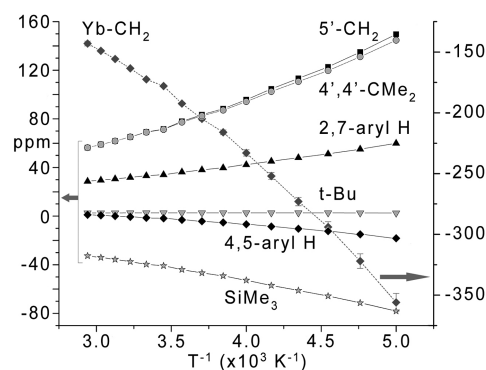


Figure 5. Variable-temperature ¹H NMR (360 MHz, toluene-*d*₈) δ vs *T*^{−1} plot over the temperature range 200–340 K for (Czx)Yb(CH₂SiMe₃)₂, **17**.

supports an electronic effect. Krogh-Jespersen and Brennan²⁰ have examined a number of mixed ligand, *mer*-octahedral lanthanide complexes and shown conclusively that anions exert a stronger *trans* influence than neutral donors in all cases.

Solution Behavior. The variable-temperature ¹H NMR spectra of the paramagnetic (Czx)Ln(CH₂SiMe₃)₂ complexes, **16** (Er) and **17** (Yb), show seven resonances in toluene-*d*₈ between 210 and 380 K, as illustrated for **17** at 250 K in Figure 4. The corresponding δ versus 1/*T* plot for **17** is shown in Figure 5. The observation of only seven resonances and reasonable straight line behavior in the δ versus 1/*T* plots is consistent with the five-coordinate, monomeric structure observed in the solid-state X-ray structures.

There is some minor curvature evident in the lines for the more shifted resonances at low temperature in Figure 5. This may be due to hindered rotation about the Ln–C bonds as the temperature is lowered since slow rotation on the NMR time scale would not result in decoalescence, assuming that the approximately C_{2v} geometry found in the X-ray structure represents the thermodynamically most favored conformation. This may also explain why the alkyl CH₂ resonance for the diamagnetic complex (Czx)Y(CH₂SiMe₃)₂, **15**, shows a small, but noticeable, temperature-dependent chemical shift (Figure 6).

The dichloride complexes **18**–**20** also show seven resonances at room temperature (cf. Figure 7). This is inconsistent with the *cis*, *mer*-geometry observed in the X-ray structures of **18**–**20**, suggesting that THF dissociation/reassociation is fast on the NMR time scale at

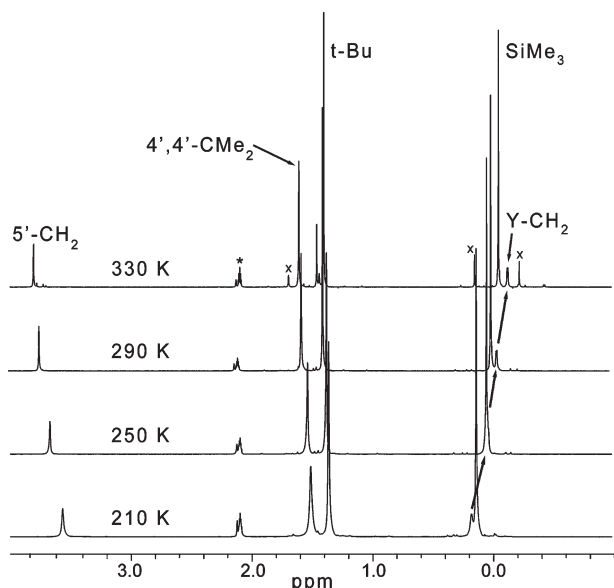


Figure 6. Variable-temperature ^1H NMR spectra (360 MHz, toluene- d_8) showing the upfield region for $(\text{Czx})\text{Y}(\text{CH}_2\text{SiMe}_3)_2$, **15** (*residual solvent resonance; \times denotes impurity growing in above room temperature).

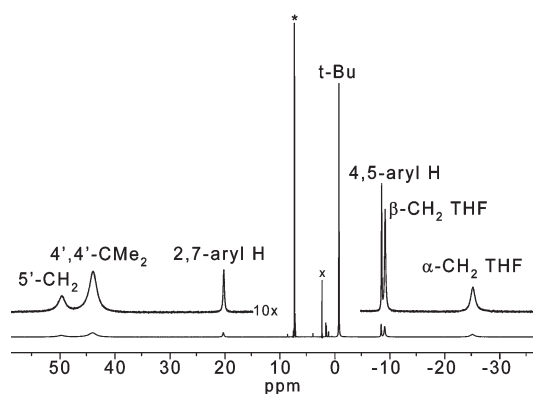


Figure 7. ^1H NMR spectrum (360 MHz, benzene- d_6) of $(\text{Czx})\text{Yb}(\text{Cl})_2(\text{THF})$, **20**, at 293 K (*residual solvent resonance; \times denotes an impurity).

this temperature for all of these complexes. However, on cooling **20**, the resonances due to the oxazoline CMe_2 and CH_2 groups each decoalesce into two new resonances with a coalescence temperature (T_c) of 272 K, as shown in Figures 8 and 9, respectively. The remaining carbazole (Figure 10) and THF (Figure 11) signals show the expected linear δ versus $1/T$ behavior down to 190 K but do not undergo decoalescence. These observations are entirely consistent with slow THF exchange from a thermodynamically favored *cis,mer* geometry (C_s symmetry) as observed in the solid-state X-ray structure. The Eyring plot for the THF exchange process, shown in Figure 12,²¹ yielded values of $\Delta H^\ddagger = 98 \pm 10 \text{ kJ mol}^{-1}$ and $\Delta S^\ddagger = +185 \pm 25 \text{ J mol}^{-1} \text{ K}^{-1}$, while a value of $\Delta G^\ddagger = 48 \pm 3 \text{ kJ mol}^{-1}$ was calculated directly from T_c .^{22,23} The observed ΔS^\ddagger is so large and positive that even recognizing the large error associated with its determination, there is little doubt the THF exchange process is dissociative. This is not entirely surprising, given the fact that we have isolated the stable five-coordinate Yb dialkyl **17**. Assuming this is a dissociative process, the measured ΔH^\ddagger value reflects the

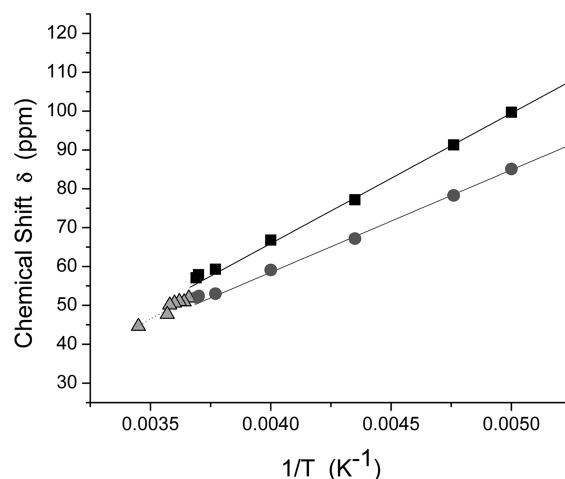


Figure 8. δ vs $1/T$ plot for the oxazoline CMe_2 ^1H NMR resonances of **20** (360 MHz, toluene- d_8 , \blacktriangle = coalesced resonance).

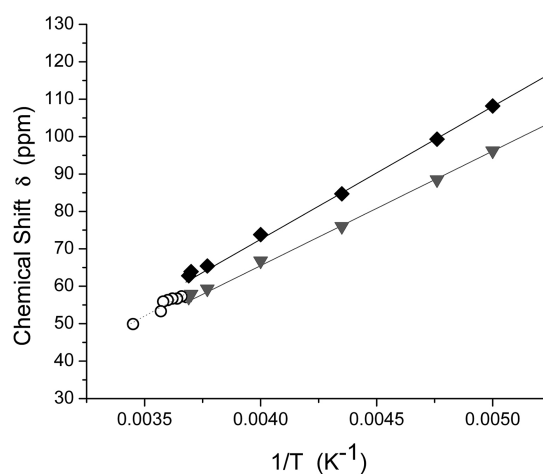


Figure 9. δ vs $1/T$ plot for the oxazoline CH_2 ^1H NMR resonances of **20** (360 MHz, toluene- d_8 , \circ = coalesced resonance).

combined THF dissociation energy and the solvent and complex reorganization energies. The previously reported Ln–THF bond strengths from experimental and theoretical studies are smaller than the ΔH^\ddagger value observed here, although they do span a very large range from 50 to 80 kJ mol^{-1} .^{24,25}

Reactivity. The dialkyl complexes **15**–**17** were initially examined as possible catalysts for the polymerization of ethylene, isoprene, and 2,3-dimethylbutadiene using $\text{Ph}_3\text{C}^+\text{B}(\text{C}_6\text{F}_5)_4^-$ (1 equiv) as activator. No polymer was observed with ethylene or isoprene, but a small amount of polymer was observed in all three cases with 2,3-dimethylbutadiene. However, since $\text{Ph}_3\text{C}^+\text{B}(\text{C}_6\text{F}_5)_4^-$ is capable of catalyzing the polymerization of 2,3-dimethylbutadiene in its own right,^{26,27} the polymerization experiments on this monomer were repeated using just slightly less than 1 equiv of $\text{Ph}_3\text{C}^+\text{B}(\text{C}_6\text{F}_5)_4^-$ as initiator. In these experiments, no poly-1,3-dimethylbutadiene was produced, confirming our suspicion that it was the trityl cation that was polymerizing 2,3-dimethylbutadiene and not any cationic alkyls derived from **15**–**17**.

Two possibilities for the lack of polymerization activity suggest themselves: either **15**–**17** do not form cationic alkyls on treatment

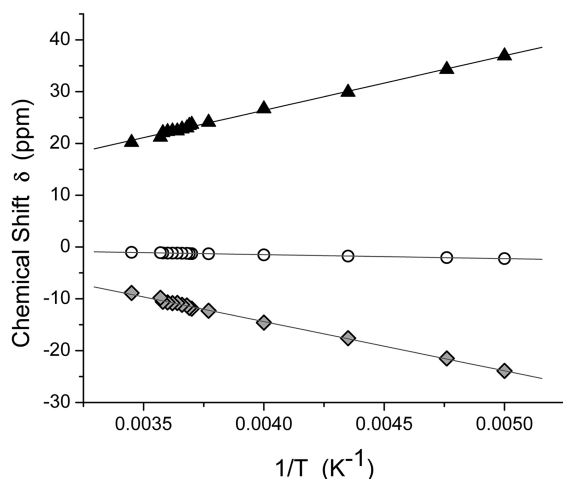


Figure 10. δ vs $1/T$ plot for the carbazole ^1H NMR resonances of **20** (360 MHz, toluene- d_8 , \blacktriangle = 2,7-carbazole H, \bullet = t-Bu, \blacklozenge = 4,5-carbazole H).

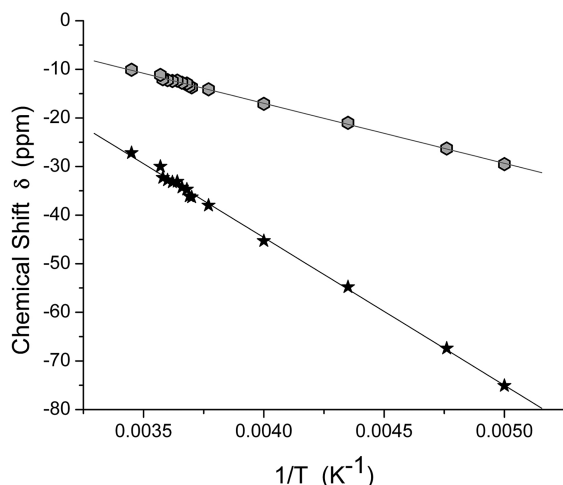


Figure 11. δ vs $1/T$ plot for the THF ^1H NMR resonances of **20** (360 MHz, toluene- d_8 , \bullet = β -THF, \star = α -THF).

with $\text{Ph}_3\text{C}^+\text{B}(\text{C}_6\text{F}_5)_4^-$ or the alkyl cations fail to insert 2,3-dimethylbutadiene at a reasonable rate. Examination of the reaction mixture formed when 1 equiv of $\text{Ph}_3\text{C}^+\text{B}(\text{C}_6\text{F}_5)_4^-$ is added to **15** in toluene- d_8 by NMR shows very clean generation of the alkyl cation **21**. The ^1H NMR spectrum is surprisingly uninformative, but the resonance for the remaining CH_2SiMe_3 group on Y now integrates to two protons ($^2J_{\text{YH}} = 2.8$ Hz vs 2.6 Hz in **15**) and the oxazoline CMe_2 group has shifted upfield to δ 1.10 ppm from 1.56 ppm in **15**. The ^{13}C NMR is more definitive however, as the CH_2 carbon directly bonded to Y shifts downfield by almost 10 ppm and the coupling constant increases by ca. 10 Hz (**21**: δ 47.80, $^1J_{\text{YC}} = 48.8$ Hz; **15**: δ 37.46, $^1J_{\text{YC}} = 38.5$ Hz). The change in $^1J_{\text{YC}}$ is consistent with a stronger and shorter Y–C bond in the alkyl cation as might be expected. Examination of the ^{19}F NMR spectrum for the $\text{B}(\text{C}_6\text{F}_5)_4^-$ anion shows a difference in chemical shift between the *meta*- and *para*-F resonances of $\Delta\delta_{\text{m,p}} = 4.4$ ppm. Differences in $\Delta\delta_{\text{m,p}}$ of more than 3.5 ppm have been taken as evidence of cation–anion association for $[(\text{PhCH}_2)\text{B}(\text{C}_6\text{F}_5)_3]^-$ anions,²⁸ but this criterion does not appear to hold very well for

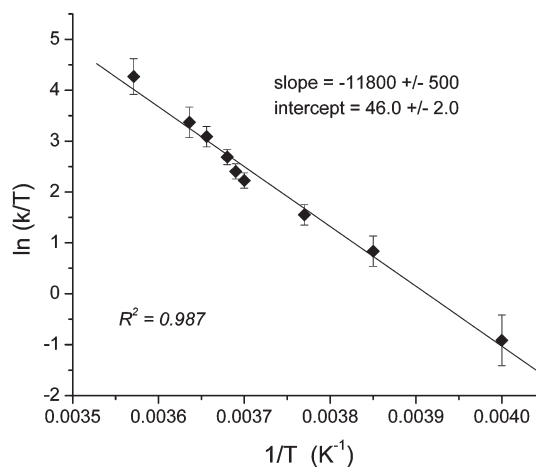


Figure 12. Eyring plot for THF exchange in complex **20**.

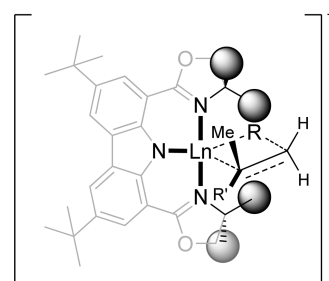


Figure 13. Crowding in the four-center σ -bond metathesis transition state for alkene insertion ($\text{R} = \text{CH}_2\text{SiMe}_3$; $\text{R}' = \text{C}(\text{Me})=\text{CH}_2$).

$[\text{B}(\text{C}_6\text{F}_5)_4]^-$ complexes since $\Delta\delta_{\text{m,p}}$ values of ca. 4 ppm has been observed both in systems where this anion is, and is not, coordinated.^{29–32} Despite the ambiguity of the $\Delta\delta_{\text{m,p}}$ values, the observation of some broadening in the ^{19}F resonances for the *ortho*- and *meta*-F of the C_6F_5 groups suggests that the anion is interacting with the cation in **21**.³² Complex **21** is stable for at least a week at room temperature in toluene- d_8 , although it decomposes on attempted isolation. We have also observed that **21** rapidly polymerizes THF when dissolved in that solvent, suggesting that the “free” alkyl cation is highly reactive.³³

The observations above unambiguously establish that alkyl cation formation occurs when **15** is treated with $\text{Ph}_3\text{C}^+\text{B}(\text{C}_6\text{F}_5)_4^-$, thus implicating slow alkene insertion as the reason **21** is inactive as a diene polymerization catalyst. The extent to which strong anion coordination is responsible for this slow insertion has not been established, but it is reasonable to assume that this is part of the problem. The failure of alkenes to insert into $\text{Ln}-\text{C}$ bonds in these complexes may also be due to the coordination geometry of the Czx ligand. Evidence presented earlier suggests that the methyl substituents on the oxazoline ring force the alkyl ligands in complexes **15**–**17** to orient themselves over the carbazole group. It seems reasonable to assume that these substituents also limit access of an alkene substrate to the metal and interfere with the four-center, σ -bond metathesis transition state since the inserting alkene must straddle the site directly opposite the carbazole N in the transition state and this region is the most crowded by the methyl groups (Figure 13). Finally, it should be noted that the NNN-donor set of the anionic carbazole-bis(oxazoline) ligand framework is strongly electron donating, and this could reduce the Lewis acidity of the

metal center and inhibit monomer coordination for electro-
nic reasons.³⁴

Preliminary experiments have also shown that **15**–**17** under-
go hydrogenolysis with H₂ under pressure to afford complex
hydrides, which may also serve as polymerization or hydrogenation
catalysts. Despite the low-reactivity catalytic activity
observed so far, we have established that the carbazole-bis-
(oxazoline) ligand system is an attractive ancillary for organo-
lanthanide chemistry, providing a well-defined *mer* geom-
etry, appropriate steric saturation, and low susceptibility to
participate in chemical reactions with either strong nucleophiles
or electrophiles.

■ ASSOCIATED CONTENT

S **Supporting Information.** Tables of atomic coordinates,
bond distances and angles, and anisotropic thermal param-
eters for **16**–**20** as well as tables summarizing comparative
X-ray structural data are available free of charge via the Inter-
net at <http://pubs.acs.org>.

■ AUTHOR INFORMATION

Corresponding Author

*E-mail: djberg@uvic.ca.

■ ACKNOWLEDGMENT

D.J.B. (Discovery Grant) gratefully acknowledges the support
of the Natural Sciences and Engineering Research Council of
Canada.

■ REFERENCES

- (1) Many reviews are available covering this area; some of the more recent reviews: (a) Xie, J.-H.; Zhu, S.-F.; Zhou, Q.-L. *Chem. Rev.* **2011**, *111*, 1713. (b) Singh, P. K.; Singh, V. K. *Pure Appl. Chem.* **2010**, *82*, 1845. (c) Framery, E.; Andrioletti, B.; Lemaire, M. *Tetrahedron: Asymmetry* **2010**, *21*, 1110. (d) Hargaden, G. C.; Guiry, P. J. *Chem. Rev.* **2009**, *109*, 2505. (e) Pfaltz, A. Bisoxazolines—a privileged ligand class for asymmetric catalysis. In *Asymmetric Synthesis*, 2nd ed.; Christian, M., Braese, S., Eds.; Wiley, VCH Verlag GmbH & Co.: Weinheim, Germany, 2008; pp 139–143. (f) Rasapan, R.; Laventine, D.; Reiser, O. *Coord. Chem. Rev.* **2008**, *252*, 702. (g) Nishiyama, H.; Ito, J.; Shiomi, T.; Hashimoto, T.; Miyakawa, T.; Kitase, M. *Pure Appl. Chem.* **2008**, *80*, 743. (h) Desimoni, G.; Faita, G.; Jørgensen, K. A. *Chem. Rev.* **2006**, *106*, 3561. (2) (a) Kobayashi, S.; Yamashita, Y. *Acc. Chem. Res.* **2011**, *44*, 58. (b) Matsunaga, S.; Shibasaki, M. *Bull. Chem. Soc. Jpn.* **2008**, *81*, 60. (c) Aspinall, H. C.; Greeves, N. J. *Organomet. Chem.* **2002**, *647*, 151. (d) Johnson, J. S.; Evans, D. A. *Acc. Chem. Res.* **2000**, *33*, 325. (e) Nishiyama, H. *Enantiomer* **1999**, *4*, 569. (3) (a) Sato, H.; Suzuki, Y.; Takai, Y.; Kawasaki, H.; Arakawa, R.; Shizuma, M. *Chem. Lett.* **2010**, *39*, 564. (b) Suga, H.; Higuchi, S.; Ohtsuka, M.; Ishimoto, D.; Arikawa, T.; Hashimoto, Y.; Misawa, S.; Tsuchida, T.; Kakehi, A.; Baba, T. *Tetrahedron* **2010**, *66*, 3070. (c) Matsumoto, K.; Suzuki, K.; Tsukuda, T.; Tsubomura, T. *Inorg. Chem.* **2010**, *49*, 4717. (d) Barros, M. T.; Phillips, A. M. F. *Tetrahedron: Asymmetry* **2010**, *21*, 2746. (e) de Bettancourt-Dias, A.; Viswanathan, S.; Rollett, A. J. *Am. Chem. Soc.* **2007**, *129*, 15436. (f) Lu, G.; Morimoto, H.; Matsunaga, S.; Shibasaki, M. *Angew. Chem., Int. Ed.* **2008**, *47*, 6847. (g) Morimoto, H.; Lu, G.; Aoyama, N.; Matsunaga, S.; Shibasaki, M. *J. Am. Chem. Soc.* **2007**, *129*, 9588. (h) Comelles, J.; Pericas, A.; Moreno-Manas, M.; Vallribera, A.; Drudis-Solé, G.; Lledos, A.; Parella, T.; Roglans, A.; Garcia-Granda, S.; Roces-Fernández, L. *J. Org. Chem.* **2007**, *72*, 2077. (i) Aspinall, H. C.; Bickley, J. F.; Greeves, N.; Kelly, R. V.; Smith, P. M. *Organometallics* **2005**, *24*, 3458. (j) Evans, D. A.;

Sweeney, Z. K.; Rovis, T.; Tedrow, J. S. *J. Am. Chem. Soc.* **2001**, *123*, 12095. (k) Desimoni, G.; Faita, G.; Filippone, M.; Mella, M.; Zampori, M. G.; Zema, M. *Tetrahedron* **2001**, *57*, 10203. (l) Qian, C.; Wang, L. *Tetrahedron: Asymmetry* **2000**, *11*, 2347. (m) Qian, C.; Wang, L. *Tetrahedron Lett.* **2000**, *43*, 2203.

(4) (a) Hong, S.; Tian, S.; Metz, M. V.; Marks, T. J. *J. Am. Chem. Soc.* **2003**, *125*, 14768. (b) Kodama, H.; Ito, J.; Hori, K.; Ohta, T.; Furakawa, I. *J. Organomet. Chem.* **2000**, *603*, 6. (c) Guillon, H.; Daniele, S.; Hubert-Pfalzgraf, L. G.; Letoffe, J. M. *Polyhedron* **2004**, *23*, 1467. (d) Alaaeddine, A.; Amgoune, A.; Thomas, C. M.; Dagonne, S.; Bellemin-Lapponnaz, S.; Carpentier, J.-F. *Eur. J. Inorg. Chem.* **2006**, 3652. (e) Gorlitzer, H. W.; Spiegler, M.; Anwander, R. *J. Chem. Soc., Dalton Trans.* **1999**, 4287.

(5) (a) Inoue, M.; Nakada, M. *Heterocycles* **2007**, *72*, 133. (b) Inoue, M.; Nakada, M. *Angew. Chem., Int. Ed.* **2006**, *45*, 252. (c) Inoue, M.; Nakada, M. *Org. Lett.* **2004**, *6*, 2977. (d) Inoue, M.; Suzuki, T.; Nakada, M. *J. Am. Chem. Soc.* **2003**, *125*, 1140. (e) Suzuki, T.; Kinoshita, A.; Kawada, H.; Nakada, M. *Syn. Lett.* **2003**, 570.

(6) (a) Durán-Galván, M.; Worlikar, S. A.; Connell, B. T. *Tetrahedron* **2010**, *66*, 7707. (b) Durán-Galván, M.; Hemmer, J. R.; Connell, B. T. *Tetrahedron Lett.* **2010**, *51*, 5080. (c) Durán-Galván, M.; Connell, B. T. *Eur. J. Org. Chem.* **2010**, 2445.

(7) (a) Gibson, V. C.; Spitzmesser, S. K.; White, A. J. P.; Williams, D. J. *J. Chem. Soc., Dalton Trans.* **2003**, 2718. (b) Hollas, A. M.; Gu, W.; Bhuvanesh, N.; Ozerov, O. V. *Inorg. Chem.* **2011**, *50*, 3673.

(8) Mudadu, M. S.; Singh, A. J.; Thummel, R. P. *J. Org. Chem.* **2008**, *73*, 6513.

(9) (a) Wang, L.; Cui, D.; Hou, Z.; Li, W.; Li, Y. *Organometallics* **2011**, *30*, 760. (b) Johnson, K. R. D.; Hayes, P. G. *Organometallics* **2009**, *28*, 6352.

(10) (a) Lappert, M. F.; Pearce, R. *J. Chem. Soc., Chem. Commun.* **1973**, 126. (b) Barker, F. K.; Lappert, M. F. *J. Organomet. Chem.* **1974**, *76*, C45. (c) Hultsch, K. C.; Voth, P.; Beckerle, K.; Spaniol, T. P.; Okuda, J. *Organometallics* **2000**, *19*, 228. (d) Clark, D. L.; Sattelberger, A. P. *Inorg. Synth.* **1997**, *31*, 307.

(11) SAINTPlus, v6.22, Data Reduction and Correction Program; Bruker AXS: Madison, WI, 2001.

(12) Sheldrick, G. M. SADABS, v2.01, Empirical Absorption Correction Program; Bruker AXS: Madison, WI, 2001.

(13) Sheldrick, G. M. SHELXTL, v6.10, Structure Determination Software Suite; Bruker AXS: Madison, WI, 2001.

(14) Farrugia, L. J. *J. Appl. Crystallogr.* **1997**, *30*, 565.

(15) Mean value and range for the Ln–C–Si bond angles in 36 reported five-coordinate (L)Ln(CH₂SiMe₃)₂ complexes. Details of the complexes and literature references are included in the Supporting Information.

(16) (a) Bondi, A. *J. Phys. Chem.* **1964**, *68*, 441. (b) Batsanov, S. S. *J. Mol. Struct.* **1999**, *468*, 151. (c) Mantina, M.; Chamberlin, A. C.; Valero, R.; Cramer, C. J.; Truhlar, D. G. *J. Phys. Chem. A* **2009**, *113*, 5806.

(17) Mean value for the Ln–C bond length in 36 reported five-coordinate (L)Ln(CH₂SiMe₃)₂ complexes, arbitrarily corrected to the ionic radius of Y³⁺ in five-coordination (0.84 Å) as given in ref 18. Details of the complexes and literature references are included in the Supporting Information.

(18) Shannon, R. D. *Acta Crystallogr. A* **1976**, *32A*, 751.

(19) Mean value for the Ln–Cl bond length in 27 reported six-coordinate (L)₂(X)Ln(Cl)₂(THF) complexes, arbitrarily corrected to the ionic radius of Y³⁺ in six-coordination (0.90 Å) as given in ref 18. Details of the complexes and literature references are included in the Supporting Information.

(20) Krogh-Jespersen, K.; Romanelli, M. D.; Melman, J. H.; Emge, T. J.; Brennan, J. G. *Inorg. Chem.* **2010**, *49*, 552.

(21) The rate constants were determined by line-shape analysis using WINDNMR: Reich, H. J. *WINDNMR* (Vers. 7.1.13); J. Chem. Educ. Software 3D2: Madison, WI, 2008. Paramagnetic line broadening results in larger than normal errors in the estimation of the rate constant *k* by this method, especially at temperatures more than 10 K above and below coalescence. However, line broadening due to exchange was still clearly observable within this window.

(22) Calculated at the coalescence temperature using the two-site, equal-population exchange formula (ref 23): $\Delta G^\ddagger = 1.912 \times 10^{-2}(T_c) - [9.972 + \log(T_c/\delta v)]$ in kJ mol^{-1} . A value of $\delta v = 1840 \text{ Hz}$ was calculated by extrapolation of the straight lines for the two inequivalent CMe_2 resonances of **20**, shown in Figure 8, to $T_c = 272 \text{ K}$. The error estimated for ΔG^\ddagger assumes a liberal error of 80 Hz in δv .

(23) Sandstrom, J. *Dynamic NMR Spectroscopy*; Pergamon: London, 1982.

(24) Ln–THF bond dissociation energies (kJ mol^{-1}): (a) $(\text{C}_5\text{Me}_5)_2\text{LuCl}(\text{THF})$, 54 (expt) Gong, L.; Streitwieser, A., Jr.; Zalkin, A. *J. Chem. Soc., Chem. Commun.* **1987**, 460. (b) $(\text{C}_5\text{H}_5)_2\text{LnX}(\text{THF})$, 50 (La), 65 (Gd), 80 (Lu) (calc): Luo, Y.; Selvam, P.; Ito, Y.; Endou, A.; Kubo, M.; Miyamoto, A. *J. Organomet. Chem.* **2003**, 679, 84. (c) $\text{Yb}(\text{BH}_4)_3 \cdot (\text{THF})_2$, 52 (expt), 54 (calc): Gafurov, B. A.; Khakerov, I. Z.; Badalov, A. B.; Mirsaidov, I. V. *Int. J. Hydrogen Energy* **2011**, 36, 1309.

(25) Closely related bond dissociation energies for comparison (kJ mol^{-1}): (a) $(\text{C}_5\text{H}_4\text{SiMe}_3)_3\text{U}(\text{THF})$, 41 (expt): Schock, L. E.; Seyam, A. M.; Sabat, M.; Marks, T. J. *Polyhedron* **1988**, 7, 1517. (b) $(\text{C}_5\text{Me}_5)_2\text{Sm}(\text{THF})$, 31 (expt): Nolan, S. P.; Stern, D. L.; Marks, T. J. *J. Am. Chem. Soc.* **1989**, 111, 7844. (c) η^6 -Arene dissociation from Yb ($\text{S-2,6-}\eta^6\text{-C}_6\text{H}_3\text{Ar}^*_2$)₂ ($\text{Ar}^* = 2,4,6\text{-C}_6\text{H}_2\text{Pr}^*_3$), 54 (expt); Yb(SH)₂-(C_6H_6)₂, 32 (calc, B3LYP) and 74 (calc, MP2): Niemeyer, M. *Eur. J. Inorg. Chem.* **2001**, 1969. (d) $(\text{Tp}^{\text{Me}_2})\text{UCl}_3(\text{THF})$, 21.5 (expt): Leal, J. P.; Martinho Simões, J. A. *J. Chem. Soc., Dalton Trans.* **1994**, 2687. (e) $\text{LaI}_3(2\text{-pyrazine})_3$ (av), 78 (calc): Mazzanti, M.; Wietzke, R.; Pécaut, J.; Latour, J.-M.; Maldivi, P.; Remy, M. *Inorg. Chem.* **2002**, 41, 2389.

(26) In a typical experiment, a 150:1 molar ratio of [2,3-butadiene]/ $[\text{Ph}_3\text{C}^+\text{B}(\text{C}_6\text{F}_5)_4^-]$ at 25 °C in toluene resulted in complete conversion to poly-2,3-butadiene within 5 min; $M_n = 1.0 \times 10^5 \text{ Da}$ and $M_w/M_n = 2.57$ (GPC using THF as solvent calibrated against polystyrene standards). Currently, we do not know whether polymerization is initiated by electrophilic addition of trityl cation or H^+ (from trace adventitious water). Several examples of polymerization by trityl cation (or H^+ derived from trace water in its presence) have been reported, ref 27.

(27) (a) Abu-Abdoun, I. I.; Ledwith, A. *J. Polym. Res.* **2007**, 14, 99. (b) Ihara, E.; Yoshida, N.; Ikeda, J.-I.; Itoh, T.; Inoue, K. *J. Polym. Sci., Part A* **2006**, 2636. (c) Tasdelen, M.; A.; Degirmenci, M.; Yagci, Y.; Nuyken, O. *Polym. Bull.* **2003**, 50, 131. (d) Acar, M. H.; Yagci, Y.; Schnabel, W. *Polym. Int.* **1998**, 48, 331. (e) Acar, M.; Küçüköner, M. *Polymer* **1997**, 38, 2829. (f) González, M.; Rodríguez, M.; León, L. M.; González, M. C.; Zamora, F. *Polym. Bull.* **1989**, 22, 163. (g) Asami, R.; Hasegawa, K. *Polym. J.* **1976**, 8, 53. (h) Asami, H.; Hasegawa, K.; Onoe, T. *Polym. J.* **1976**, 8, 43. (i) Slomkowski, S.; Kubisa, P.; Penczek, S. *Nuova Chim.* **1973**, 49, 51.

(28) Horton, A. D.; de With, J. *Organometallics* **1997**, 16, 5424.

(29) Coordinated $[\text{B}(\text{C}_6\text{F}_5)_4]^-$ anion: Zuccaccia, C.; Stahl, N. G.; Macchioni, A.; Chen, M.-C.; Roberts, J. A.; Marks, T. J. *J. Am. Chem. Soc.* **2004**, 126, 1448 ($(\text{C}_5\text{Me}_5)_2\text{Th}(\text{CH}_3)(\text{B}(\text{C}_6\text{F}_5)_4)$, $\Delta\delta_{\text{m,p}} = 3.89 \text{ ppm}$).

(30) Noncoordinated $[\text{B}(\text{C}_6\text{F}_5)_4]^-$ anion: (a) Ref 27 ($[\text{C}_5\text{Me}_4\text{-SiMe}_2\text{NBu}^1]\text{Zr}(\text{CH}_3)(\text{THF})^+[\text{B}(\text{C}_6\text{F}_5)_4]^-$, $\Delta\delta_{\text{m,p}} = 4.00 \text{ ppm}$). (b) Li, D.; Li, S.; Cui, D.; Zhang, X.; Trifonov, A. *J. Chem. Soc., Dalton Trans.* **2011**, 40, 2151. ($[(\text{NacNac})\text{Sc}(\text{CH}_2\text{SiMe}_3)]^+[\text{B}(\text{C}_6\text{F}_5)_4]^-$, $\Delta\delta_{\text{m,p}} = 3.83 \text{ ppm}$ and directly compared with $[\text{Ph}_3\text{C}]^+[\text{B}(\text{C}_6\text{F}_5)_4]^-$, $\Delta\delta_{\text{m,p}} = 3.96 \text{ ppm}$, both in C_6D_6 solution.)

(31) (a) Alonso-Moreno, C.; Lancaster, S. J.; Wright, J. A.; Hughes, D. L.; Zuccaccia, C.; Correa, A.; Macchioni, A.; Cavallo, L.; Bochmann, M. *Organometallics* **2008**, 27, 5474. (b) Bryliakov, K. P.; Talsi, E. P.; Voskoboinikov, A. Z.; Lancaster, S. J.; Bochmann, M. *Organometallics* **2008**, 27, 6333.

(32) Jia, L.; Yang, X.; Stern, C. L.; Marks, T. J. *Organometallics* **1997**, 16, 842.

(33) Although $[\text{Ph}_3\text{C}]^+[\text{B}(\text{C}_6\text{F}_5)_4]^-$ can also polymerize THF, the same reactivity was observed when less than 1 equiv of the trityl borate was used, so we believe it is actually **21** that initiates the polymerization of THF in this case.

(34) The authors wish to thank a referee for pointing this possibility out.